



HAL
open science

Cellular pathways controlling integron cassette site folding

Céline Loot, David Bikard, Anna Rachlin, Didier Mazel

► **To cite this version:**

Céline Loot, David Bikard, Anna Rachlin, Didier Mazel. Cellular pathways controlling integron cassette site folding. *EMBO Journal*, 2010, 29 (15), pp.2623-2634. 10.1038/emboj.2010.151 . pasteur-02477658

HAL Id: pasteur-02477658

<https://pasteur.hal.science/pasteur-02477658>

Submitted on 1 Apr 2020

HAL is a multi-disciplinary open access archive for the deposit and dissemination of scientific research documents, whether they are published or not. The documents may come from teaching and research institutions in France or abroad, or from public or private research centers.

L'archive ouverte pluridisciplinaire **HAL**, est destinée au dépôt et à la diffusion de documents scientifiques de niveau recherche, publiés ou non, émanant des établissements d'enseignement et de recherche français ou étrangers, des laboratoires publics ou privés.



Distributed under a Creative Commons Attribution - NonCommercial 4.0 International License

Cellular pathways controlling integron cassette site folding

Céline Loot, David Bikard, Anna Rachlin¹ and Didier Mazel*

Institut Pasteur, Unité Plasticité du Génome Bactérien, CNRS URA2171, Paris, 75724, France.

*Correspondence: mazel@pasteur.fr

¹ Present adress: McLean Hospital, Behavioural Genetics Lab, MRC 215, Mill St Belmont, MA 02478, USA.

Character number: 45570

Running title: Integron recombination

Subject category: Genome stability & Dynamics, Microbiology & Pathogens

ABSTRACT

By mobilizing small DNA units, integrons play a major role in the dissemination of antibiotic resistance among bacteria. The acquisition of gene cassettes occurs by recombination between the *attI* and *attC* sites catalyzed by the IntI1 integron integrase. These recombination reactions use an unconventional mechanism involving a folded single-stranded *attC* site. We show that cellular bacterial processes delivering single-stranded DNA, such as conjugation and replication, favour proper folding of the *attC* site. We also provide evidence that DNA superhelicity allows *attC* sites to extrude from double-stranded DNA as cruciform structures *in vitro* and *in vivo*. We demonstrate that the proper folding of the *attC* site depends on both the propensity to form non-recombinogenic structures and the length of their variable terminal structures. These results draw the network of cell processes that regulate integron recombination.

Keywords: cruciform/integron/recombination/single-stranded DNA/superhelicity

INTRODUCTION

Integrations are genetic elements commonly found in bacteria from diverse phyla and environments (Mazel, 2006). They are defined as gene capture systems which incorporate exogenous open reading frames and convert them to functional genes by ensuring their correct expression (Hall and Collis, 1995). The integron platform consists of three major elements: an *intI* gene coding a site-specific recombination enzyme belonging to the tyrosine-recombinase family (Azaro and Landy, 2002) called an integrase, a primary recombination site (*attI*), and an outward oriented promoter (P_c) which directs transcription of captured gene cassettes (Hall and Collis, 1995). Gene cassettes generally contain a single gene and an imperfect inverted repeat at the 3' end called an *attC* site. Recombination events between the *attI* and *attC* sites, leading to the insertion of gene cassettes in the platform, are the most common and efficient reactions performed by integron-associated integrases (Collis et al., 2001).

The length of natural *attC* sites varies from 57 to 141bp. They include two regions of inverted homology, R''-L'' and L'-R', that are separated by a central region that is highly variable in length and sequence (Stokes et al., 1997) (Figure 1A). Contrasting with their sequence heterogeneity, the *attC* sites display a strikingly conserved palindromic organization (Hall et al., 1991; Rowe-Magnus et al., 2003; Stokes et al., 1997) that can form secondary structures through the self-pairing of DNA strands. Upon folding, single-stranded (ss) *attC* sites present an almost canonical core site consisting of R''-R' and L''-L' duplexes separated by an unpaired central segment (UCS), two or three extrahelical bases (EHB) and a variable terminal structure (VTS) (Bouvier et al., 2009). The VTSs vary in length among the various *attC* sites from 3 predicted unpaired nucleotides such as for *attC_{aadA7}*, to a complex branched

secondary structure in the larger sites such as the VCRs (*Vibrio cholerae attC* sites, Figure 1B).

It has been shown using a DNA binding assay that IntI1 binds strongly and specifically to the bottom strand (bs) of ss *attC* DNA (Francia et al., 1999). *In vivo*, it has also been shown that only the bs of the *attC* site is used as a substrate during the integration of gene cassettes (Bouvier et al., 2005) thereby creating a pseudo-Holliday Junction (pHJ) between the ss *attC* and the double-stranded (ds) *attI* site. It is currently believed that this pHJ is resolved through host processes, but these have yet to be identified.

Many questions about the specific nature of these unique gene capture systems still remain unanswered. Specifically, we do not yet know how and when the *attC* sites fold inside the cell, or the identity of the factors influencing these processes.

It has long been clear that structures more complex than the canonical double helix B-form DNA are biologically important. These include unpaired or mismatched bases, triplex DNA, Z-form DNA, hairpin loops, cruciforms and Holliday junctions (Bacolla and Wells, 2004). DNA secondary structures have been detected in both prokaryotes and eukaryotes and can be assembled essentially by two pathways: from a single-stranded DNA by generating a hairpin structure or from double-stranded DNA by extrusion of cruciform structures (Figure 2).

The first pathway requires single-stranded DNA, which can be produced during conjugation, natural transformation, viral infection, replication, transcription and DNA repair. Here, we examined the effect of ss availability mediated by two cellular processes considered as the principal sources of ss DNA in bacterial cells, conjugation and replication (Figure 2). During conjugation, the transferred DNA is in essence single-stranded, while during replication, the lagging strand contains a region of ss DNA reflecting the length of an Okazaki fragment (1 to 2kb). These may therefore provide an opportunity for the formation of DNA

secondary-structure. Our results show that the availability of ss DNA in the cell during conjugation and/or during replication (lagging strand) could favour the folding, and thus recombination, of *attC* sites of various lengths. However, the results could not be fully explained by these ss DNA production pathways, suggesting that other processes are likely involved. We thus considered the possibility that *attC* sites could be extruded from double strand DNA into a cruciform structure (Figure 2). The formation of a cruciform by an inverted repeat involves a great deal of structural disruption since it requires a complete reorganisation in base-pairing. Furthermore, superhelicity is expected to directly influence cruciform extrusion. We tested this possibility as a second *attC* folding pathway, and found that the *attC* sites could recombine from DNA essentially under ds form, after extrusion of the cruciform structure in a superhelicity-dependant manner. We confirmed these results by *in vitro* cruciform detection. We also showed that two parameters are implicated in the proper folding of the bs of the *attC* site: the length of the VTS and the propensity of the *attC* site to form a non-recombinogenic structure. Our results suggest that the contribution of these different processes varies as a function of the length and the sequence of the *attC* sites.

These results show that ss DNA structures, be they generated from replication, conjugation or extruded from ds DNA, can be recruited for specific processes such a site-specific recombination. The interplay between these cellular processes governs folding of *attC* sites, and certainly allows regulation of integron recombination by the host.

RESULTS

Influence of single strand DNA availability during conjugation on *attC* folding

We have previously shown using a conjugation based assay that the *attC* sites, contrarily to the *attI* sites, recombine as a folded ds structure generated from the ss bottom strand of the *attC* site (Bouvier et al., 2005). Conjugation proceeds exclusively via ss DNA transfer and thus is ideal to determine the folding constraints from fully single-stranded substrates.

Natural *attC* sites sizes vary from 57 to 141 nt. In order to determine if these limits correspond to ss DNA constraints, we made a series (21) of *attC* site derivatives (Figure S1, Table S1 and S2). Starting from the VCR_{2/1} (the 123 bp signature *attC* site of the *V. cholerae* superintegron), we increased the length of the stem and/or VTS (up to sites of 180 nt). Inversely, we serially deleted the central part of the VCR_{2/1} site to make shorter derivatives (down to 56 nt). Three wild type *attC* sites were also tested: *attC_{aadA7}*, *attC_{ereA2}* and *attC_{oxa2}*. We first tested them in the suicide conjugation assay we previously developed (Bouvier et al, 2005). This assay uses conjugation to deliver the *attC* site in ss form to a recipient cell expressing the IntI1 integrase and carrying the *attI* recombination site. The *attC* site provided by conjugation is carried on plasmid, pSW that cannot replicate in the recipient. This system permits the delivery of DNA in ss form to provide a substrate for recombination. We verified that all the constructed pSW::*attC* plasmids were transferred at similar rates ($\sim 3 \times 10^{-1}$) using a recipient strain able to sustain pSW replication.

The results are shown in Figure 3A. Recombination frequencies are plotted as a function of the probability of the *attC* site to fold into a recombinogenic site. We define a recombinogenic site as forming the R'/R'' box as well as having the G16 extrahelical base of the L box. The UNAFold software was used to estimate the probability to form active sites. We observed that the recombination frequencies tended to drop for sites with very low probabilities to fold properly. Nevertheless, most of the *attC* sites displayed similar

recombination frequencies when delivered by conjugation, regardless of their size or VTS length (Figure S1 and Table S3). This was in agreement with Bouvier et al., 2009.

These results suggested that if an upper limit to the length of *attC* sites exists, it is not constrained by the availability of ss DNA during conjugation.

In a second set of experiments, we compared the recombination frequencies of the *attC* sites when the bottom or the top strand was injected into recipient cells that either could or could not sustain their replication. Four natural *attC* sites were tested: VCR_{2/1}, *attC*_{aadA7}, *attC*_{oxa2} and *attC*_{ereA2}. They were all cloned into the pSW::*attC*-B and pSW::*attC*-T plasmids which permit the delivery of the bottom and the top strand respectively, through conjugation (Bouvier et al., 2005). As previously observed, when the top strand of the *attC* site was injected into a [*pir*-] recipient strain, we obtained a much lower recombination frequency (Figure 3B). This confirmed that the *attC* sites are essentially ss in this assay. If they were not, one would expect similar recombination frequencies for the top and the bottom strand (Bouvier et al., 2005). We then performed the same experiment using a *pir*+ recipient cell that permitted the replication of the pSW::*attC* substrate once transferred. In these conditions, we observed for both pSW::*attC*-B and pSW::*attC*-T plasmids an equivalent high efficiency of recombination (Figure 3B). This suggested that replication can induce recombination at a similar or higher frequency than conjugation, bringing the recombination frequencies of the two transferred strands in this assay to the same level.

We conclude that recombination can happen both during the delivery of ss DNA (the bottom strand) by conjugation and from other processes involving a replicating molecule. Recombination may indeed occur during replication-mediated DNA melting and/or during the extrusion of the *attC* site in a cruciform structure from ds DNA.

Influence of single-strand DNA availability during replication on *attC* folding

Replication is a process that transiently produces ss DNA. This in turn could regulate folding of the *attC* site (Figure 2). Based on the differences in the dynamics between the lagging and leading strands during DNA replication, proper *attC* folding is probably favoured by its localization on the lagging strand where large regions of ss DNA are available (the length of the Okazaki fragment: 1 to 2 kb, (Trinh and Sinden, 1991)). If there are differences in recombination frequency based on which strand the *attC* is on, this would support the theory that the bottom strand can be folded independently of the top strand as a hairpin structure.

To test this hypothesis, we inserted an *attC* site (either *attC_{aadA7}* or *VCR_{2/1}*) in both orientations into a unidirectional replicating pTSC plasmid, so that the bottom strand of the *attC* site is either on the leading or on the lagging strand. For the purpose of the experiment the origin of replication is thermosensitive (ori_{pSC101ts}) (Table S1). These pTSC::*attC* plasmids were introduced into strain UB5201 with two other plasmids, one containing the *attI* site (pSU38Δ::*attI*) and the other carrying the *intI1* gene (pBAD::*intI1*). Assays were performed at 30°C in presence of arabinose ensuring the expression of the integrase gene. Recombination events between *attI* and *attC* sites were then selected on plates at 42°C with the pTSC::*attC* plasmid resistance marker (Cm). At 42°C, the temperature sensitive pTSC::*attC* plasmids are unable to replicate and therefore cells containing these plasmids do not grow on Cm, unless there was a recombination event producing a cointegrate between the pTSC::*attC* and pSU38Δ::*attI* plasmids. Results are shown in Figure 3C. We obtained for pSW::*attC_{aadA7}* and pSW::*VCR_{2/1}* a 4.2 and 12.1-fold increase in recombination respectively when the bottom strand of these *attC* sites corresponds to the lagging strand. As a control, the same experiment was performed on a bidirectional replicating plasmid. As expected, we did

not observed any significant differences between the two orientations for the *attC* site (data not shown).

Remarkably, there was still a high rate of recombination when bottom strands of *attC_{aadA7}* and *VCR_{2/1}* were carried on the leading strand (respectively 1.14×10^{-1} and 1.96×10^{-3} , Figure 3C). Very little ss DNA is produced on the leading strand, making hairpins unlikely to fold. This led us to suspect another pathway.

Finally, these results show that ss production in both conjugation and replication influence and favour folding of the *attC* site, but other mechanisms are implicated. Specifically, we then studied the ability of the *attC* sites to extrude from ds DNA as cruciform structures able to recombine (Figure 2).

Influence of double strand and single strand DNA availability on *attC* folding

We used all previously tested *attC* sites derivatives (Figure S1) in the replicative condition assay. Contrarily to the conjugation assay, *attC* sites are provided on a replicative plasmid and are thus mostly double-stranded over the cell cycle, being only transiently single-stranded during replication. In these conditions, the various sites display markedly different recombination frequencies (Table S3). We observe a correlation between the VTS length and the recombination frequency (Figure 4A); *attC* sites containing a minimal VTS (3 nt) recombined at a frequency ranging from 1.01×10^{-1} (*VCR_{GC}*) to 3.53×10^{-1} (*attC_{aadA7}*), while *attC* sites containing a larger VTS recombined at a lower frequency, from 4.37×10^{-5} (*VCR_{147c}*) to 1.01×10^{-2} (*VCR_{116b}*). A negative effect of the VTS length on recombination is in agreement with the hypothesis of cruciform formation. Indeed, to go from a double-stranded state to a cruciform, an *attC* site needs to melt at least the length of its VTS (see Discussion).

The energy to melt this region can thus be considered as the energy of activation of cruciform formation, and thus is directly correlated to the probability of forming a cruciform following the Arrhenius equation (Figure S2). Therefore, the larger the VTS is, the lower the probability of folding into a cruciform, which is what we observed. Furthermore, we found that the propensity of the *attC* site to form non-recombinogenic secondary structures directly impacts the recombination frequency. This is illustrated in Figure 4B which represents the most favorable structure for the two “a” and “b” versions of VCR₉₇. The “a” and “b” versions only differ by a few bases substitutions in the VTS but these point mutations modify the formation of improperly folded structures. Indeed, the most favorable structure formed by VCR_{97a} differs greatly from the active one and thus has a very low probability of being an active substrate for recombination. On the other hand, the most stable structure for VCR_{97b} is very similar to that of the active site. It might even be recognized by the integrase which could help reach the active conformation. Not surprisingly, VCR_{97a} has a 20-fold lower recombination frequency than VCR_{97b}. The same effect of non-recombinogenic structures can also explain the 40-fold difference between the VCR_{116a} and VCR_{116b}.

It thus seems that two main parameters are instrumental for the recombination frequency of *attC* sites in these conditions. First, the longer the VTS is, the lower the recombination frequency. Second, the accumulation of non-recombinogenic (improperly folded) sites dilutes the number of active (properly folded) sites available for recombination. Note that these two parameters are not independent, as the longer is the VTS, the higher is the chance to form stable non-recombinogenic structures. An analysis of covariance performed with these two regressors (the length of the VTS and the probability of folding properly) explains 82.5% (R^2) of the experiment variance with a p-value of 4.72×10^{-9} , confirming the implication of these two parameters.

This, combined with the fact that high recombination frequencies can be obtained in replicative conditions when the bs of the *attC* site is on the leading strand of replication, strengthens the hypothesis that recombination can occur with *attC* sites that are extruded as cruciform structures.

Detection of *attC* cruciform structures

In order to test if the *attC* sites could be directly extruded as cruciform structures from a ds DNA molecule, we performed complementary *in vitro* and *in vivo* analysis.

- In vitro Mapping of S1 Nuclease-Sensitive Sites

Inverted repeat sequences in natural plasmids and phages have been shown to be centrally hyper-sensitive to cleavage by single strand selective nucleases (Lilley, 1980; Panayotatos and Wells, 1981). Indeed, when folded into hairpins, they exhibit not only ss DNA in their loop but also in potential bulges of their stem. S1 nuclease, which cleaves single-stranded DNA, was previously used to probe the formation of cruciform structures *in vitro* (Noirot et al., 1990). We carried out the same kind of experiments to detect *in vitro* formation of *attC* cruciform structures. The method consists of treating supercoiled plasmid DNA containing the *attC* sites with S1 nuclease. This is followed by a restriction digest with an enzyme having a single site in the molecule, which produces pairs of fragments arising from molecules linearized by S1 nuclease. Restriction enzymes used and expected band sizes (corresponding to the cruciform detection) are mentioned in figure 5A. This assay showed that cruciform formation was occurring at detectable rates from the *attC_{aadA7}* site, but not from the VCR_{2/1} site (Figure 5B). These results coincided with the fact that *attC_{aadA7}* has a very

short VTS (3 nt) relative to that of VCR_{2/1} (61 nt), allowing cruciform extrusion at a much higher frequency. These results paralleled the high recombination frequency of *attC*_{*aadA7*} in “replicative” conditions.

- *Recombination from ds plasmid*

In the “replicative” assay described above, the *attC* site is carried by a ds DNA plasmid able to replicate and therefore transiently produce ss DNA. To precisely study the ability of the *attC* site to recombine as a cruciform structure, we developed an assay ensuring the delivery of the *attC* site from exclusively ds DNA. For this, Π - dependant plasmids containing the *attC* sites were introduced by transformation in *pir*- deficient strains. These plasmids cannot be selectively maintained without recombination to an independent replicon. We found that all tested *attC* sites could lead to detectable cointegrate formation through recombination with the *attI* site, although the efficiency was variable (Figure 5C). These results strongly suggest that the *attC* site can extrude from double-stranded DNA as a cruciform. However, part of the difference can certainly be explained by the formation of non-recombinogenic structures. This is illustrated by comparison of the recombination frequencies and the energy landscapes of VCR_{2/1} and *attC*_{*aadA7*} (Figure 5D). An improperly folded structure for the natural VCR_{2/1} site is clearly visible (blue color shifted from the middle of the base of the triangle) and correlates with its relatively low recombination frequency. In contrast, the most efficient site, *attC*_{*aadA7*}, presents a very favorable energy landscape to fold as a recombinogenic site (blue color from the middle). Here again, both the length of the VTS and the propensity to fold into non-recombinogenic structures seem to explain the recombination frequencies of the *attC* sites. As these results strongly suggested that substrate *attC* sites could be formed by cruciform extrusion from ds DNA, we tested the effect of superhelicity on the recombination of *attC* sites under ds DNA form.

The influence of superhelicity on integron recombination

Cruciform extrusion requires the opening of the DNA double helix to allow intra-strand base pairing. The free energy held by the supercoiled molecule in the form of torsional underwinding is required for stabilization of cruciforms (Lilley et al., 1985). We first tested the effect of supercoiling on *attC* cruciform extrusion *in vitro*. Topoisomerase I, which catalyzes the relaxation of negatively supercoiled DNA by introducing single strand breaks that are subsequently religated, is supposed to prevent cruciform extrusion. As expected, we observed an inhibitory effect of topoisomerase I treatment on recombination, confirming *attC_{aadA7}* cruciform extrusion *in vitro* (Figure 6A).

Secondly, to investigate the influence of supercoiling on the *attC* site folding *in vivo*, we used negatively coiled and relaxed plasmids to transform a JTT1 WT strain containing the *attI* site and expressing the integrase. We followed the experimental procedure described above. Negatively coiled plasmids appear to recombine 2.8 times better than plasmids that are relaxed (Figure 6B). However in this experiment, the topoisomerases and gyrases of the WT strain could act on the transformed plasmids before their recombination and could thus blunt the effect of supercoiling. Therefore, we repeated the experiment in the strain SD7, a *topA10 gyrB266* derivative of JTT1, which due to its mutations in topoisomerase I and DNA gyrase, has lower levels of supercoiling than the wild-type. It has been previously established using a pUC19 plasmid, that the average superhelical density ($-\sigma_{av}$) in the JTT1 and SD7 strains was 0.057 and 0.049, respectively (Napierala et al., 2005). In SD7, the recombination ratio between supercoiled and relaxed plasmids was found to be 3.9 times higher (Figure 6B). Thus superhelicity directly affects integron recombination, supporting the cruciform extrusion pathway for *attC* site recombination.

DISCUSSION

DNA secondary structures

Extensive studies of DNA secondary structure during the past decades have shown that DNA is a dynamic molecule whose structure depends on the underlying nucleotide sequence and is influenced by the environment and the overall DNA topology. Several non-B-DNA structures have been described (Z-DNA, triplex DNA, unpaired DNA bases and hairpin or cruciform structures), which are stabilized by negative supercoiling and can be formed under physiological conditions. Circumstantial evidence suggests that cruciform structures may serve functional roles in processes such as transcription regulation (Dai and Rothman-Denes, 1999; Hartvig and Christiansen, 1996), conjugation (Guasch et al., 2003), initiation of replication (Khan, 2005) or replication slippage (Bierne et al., 1997; d'Alencon et al., 1994). More recently, it has been shown that secondary structures are implicated in the recombination of genetic elements. Indeed, Xer recombinases can promote the direct integration of the (+)ssDNA genome of CTX into the double-stranded *dif* site of *V. cholerae*. ssDNA substrates for integration can fold into a stem-loop structure, creating a small region of duplex DNA that is the target of site-specific recombinases (Val et al., 2005). Secondary structures are also implicated in the transposition of IS608 of *Helicobacter pylori*, where the TnpA transposase recognizes and cleaves only the top strand of the IS608 ends that have folded into hairpin structures (Guynet et al., 2008; Ton-Hoang et al., 2005).

In the integron recombination process, the *attC* site is recognized by the integrase as a single-stranded folded substrate (Bouvier et al., 2005; Bouvier et al., 2009, Frumerie, 2009 #2764; Frumerie et al., 2009; MacDonald et al., 2006). To adopt this structural state the DNA double helix needs the opening of inter-strand base pairing. As analysis of the integrase protein sequence failed to identify any helicase domain, we proposed that folding of the *attC*

site could either be spontaneous and energy driven in supercoiled DNA, or could be driven by host factors. In this study, we focused our attention on the folding process for *attC* sites and tested the contribution of the two pathways that can be involved: hairpin formation linked to single strand availability and/or a cruciform extrusion from supercoiled ds DNA.

Single strand availability

Single strand DNA production is obviously the most straightforward process allowing the folding of DNA into secondary structures. ss DNA is central for most examples of horizontal gene transfer. During natural transformation of bacteria, one DNA strand is taken up into the cytoplasm while its complementary strand is degraded. During conjugation, ss DNA is unwound from the duplex plasmid and transferred into the recipient bacterium. During transduction, filamentous phages such as M13, MV-L51 or Φ X174 are known to inject ssDNA. Inside the cell, there are essentially three processes that create ss DNA, replication, repair and transcription. During transcription, the size of the ss DNA is limited by the maximal size of the transcription bulge (25 nt) (Gamper and Hearst, 1982), and is likely not implicated in *attC* folding, since this size is too small. During DNA repair, the processing of double strand breaks by the RecBCD complex is a significant source of RecA nucleofilaments, (ie the assemblage of RecA monomers on ss DNA) (Spies et al, 2005). Replication seems very appropriate to favour DNA secondary structures. During this process, after the melting of ds DNA by the replication machinery, an asymmetric fork is created where one of the two strands (the lagging strand) provides a large quantity of ss DNA. Published observations suggest that secondary structures are easily made when carried on the lagging strand (Trinh and Sinden, 1991).

We carefully analyzed how conjugation and theta replication allow the bs of the *attC* site to fold and thus influence integron recombination. We showed that conjugation ensures the

folding of *attC* sites containing a longer VTS (e.g. VCR) or a shorter VTS (e.g. *attC_{aadA7}*) with even efficiency. We also demonstrate that when carried on the lagging strand of the replicated DNA, the *attC* bs is recombined at higher rate, showing that the availability of ss DNA impacts the recombination frequency of *attC* sites. These results on the influence of replication on *attC* folding led us to examine the orientation of *attC* sites on all the chromosomal integrons encountered in sequenced bacterial genomes. We observed that the bs of all *attC* sites were located on the leading strand (Figure S3). This specific orientation of *attC* sites could limit cassette rearrangements in chromosomal integrons. Nevertheless, it has been shown that DNA damage can uncouple the replication of the leading and lagging strand forming a partially ds molecule with a ss region of about 1kb on the leading strand (Pages and Fuchs, 2003).

Double strand extrusion

DNA sequences that possess two-fold symmetry may re-organize their base pairing to form cruciform structures, in which there is local intra-strand hydrogen bonding (Lilley, 1980). Nevertheless, cruciforms are intrinsically less stable than the unbranched duplex DNA from which they are derived. Supercoiling provides free energy that may be employed to stabilize unstable structural polymorphs. We studied *attC* folding as a cruciform structure and the implication of supercoiling in integron recombination. We monitored *in vitro* cruciform formation by detection of changes in nuclease sensitivity caused by the formation of these structures. We also presented an *in vivo* study that demonstrates the ability of *attC* sites to extrude from ds DNA as cruciform structures. The most conclusive assay is the transformation of supercoiled pSW::*attCs* plasmids into a recipient strain where they cannot replicate. The *attC* sites are carried by ds DNA and would mostly recombine after cruciform

extrusion. We obtained in these conditions a significant recombination frequency for all the tested *attC* sites. Using a series of VCR derivatives, we showed that proper *attC* site folding depends on two parameters in replicative conditions: the length of the VTS and the propensity to form non-recombinogenic structures. It is important to note that in the conjugation assay, these two parameters do not seem to influence integron recombination, probably due to the fact that the *attC* sites are exclusively delivered as ss DNA.

We also studied the influence of superhelicity on *attC* folding. The dynamic balance between the activities of DNA gyrase and DNA topoisomerase I maintains the level of supercoiling in *E. coli* (Lodge et al., 1989; Pruss and Drlica, 1986). Therefore, by using topoisomerase I and gyrase-deficient strains, as well as *in vitro* topoisomerase I-treated plasmids, we demonstrated a significant effect of supercoiling on proper *attC* folding and recombination.

S-type and C-type cruciform kinetics of extrusions

There are two alternative pathways by which inverted repeat sequences may extrude cruciform structures from supercoiled DNA molecules. S-type cruciforms, which are more common, are characterized by lower activation parameters (about four time less) than for C-type cruciforms (Lilley et al., 1985). The mechanism proposed for S-type extrusion involves a small initial opening of basepairs (~10 bps) limited to the centre of the inverted repeat, allowing intra-strand basepairing and formation of a four-way junction, with branch migration forming the fully extruded cruciform. C-type species proceed via a large unpaired region, covering at least the entire inverted repeat, which then forms the fully extruded cruciform in a single event of hairpin formation. The extrusion process is determined by the nature of the sequences that form the context of the inverted repeat. For *attC* sites that present a long VTS such as VCR_{2/1}, the C-type cruciform pathway is probably favoured whereas for *attC* sites with a very short VTS such as *attC*_{aadA7}, *attC*_{ereA2} and *attC*_{oxa2}, the S-type cruciform pathway

could be preferential (Figure 7). C-type kinetics are conferred by A+T rich sequences. Remarkably, we can observe differences of the A+T content between the genes cassettes of several integrons. Indeed, an average A+T content of 59.3% is observed for the gene cassette arrays of *Vibrio* sp. isolate DAT722 (VCR with large VTS), whereas the A+T content of the cassette arrays of the *Xanthomonas* strain collection ranged from 42.2% to 52.3% (*attC* sites with small VTS) (Boucher et al., 2006). A higher A+T rich content of *Vibrio* superintegron could ensure the folding of the VCR sites with large VTS by the C-type pathway.

About the constraints of the natural sites

Sites like *attC_{aadA7}* seem evolutionarily optimized since they display very favorable folding. On the contrary, the VCR sites display large VTS and non-recombinogenic structures hindering recombination.

In addition to those constraints exerted on the *attC* sites for their efficient folding, we found that their propensity to accumulate mutations could also affect their upper length limit (141 bp for *attC_{qacE}* (Stokes et al., 1997)). Indeed, during the construction of the VCR₁₈₀ site, we obtained a much higher proportion of mutations than with the smaller sites. Long palindromes pose a threat to genome stability by hindering passage of the replication fork. It is known that cells have evolved a post-replicative mechanism for the elimination and/or repair of large DNA secondary structures employing the SbcCD endonuclease (Leach, 1994). Thus for the larger sites, if they can fold well, they would hinder replication and thus be unstable. Conversely, large sites that fold poorly would have recombination frequencies too low to be selected.

Folded *attC* sites as sensors of environmental stress

Cruciforms have lower thermodynamic stability than regular duplex DNA. They have been observed only in negatively supercoiled molecules, where the unfavorable free energy of formation is offset by the topology of the torsionally stressed molecule. This can be a disadvantage, as cruciform structures can be observed only in relatively large supercoiled DNA circles, and are destabilized when a break is introduced at any location. Thus integron recombination is not only controlled by all the processes which produce ss DNA (conjugation, transformation, replication...) but also by those implicated in the variation of DNA topology. In *E. coli*, superhelicity has been shown to vary considerably during cell growth, and to change in different growth conditions (Balke and Gralla, 1987; Jaworski et al., 1991). The level of superhelicity can also vary between bacterial strains. For example, the average supercoil density for mid-log cultures of WT *Salmonella* ($\sigma=-0.060$) is 13% lower than that for *E. coli* ($\sigma=-0.069$) (Champion and Higgins, 2007). Hence, changes in supercoiling in response to external and internal stimuli could play a significant role in the formation and stability of cruciform *attC* sites. Along this line, it would be interesting to investigate the relation between stress and coiling state.

Recently, it has been shown that in *Streptococcus pneumoniae*, a gram+ bacterium, competence and therefore single strand production is induced by an antibiotic stress response (Prudhomme et al., 2006). In *Bacillus subtilis*, the competence state has been found to be required for the cell to revert point mutations in auxotrophic alleles when grown on minimal medium (Robleto et al., 2007). These are two examples where single-stranded DNA production is triggered in response to stress conditions.

This novel concept for regulating the recombination of gene cassettes in integrons appears to be of considerable importance, since filamentous phages (Val et al., 2005) and insertion sequences (Ton-Hoang et al., 2005) also use this mobilization mechanism. It was recently shown that integron-mediated recombination is integrated with the SOS response

(Guerin et al., 2009), which in turn is activated by the production of the substrate for integron-mediated recombination - ssDNA. The use of this unconventional form of DNA as substrate allows another level of regulation in the integron recombination process. The results presented here confirm the position of integrons as an integrated adaptive system and strengthen the role of single-stranded DNA as sensors of environmental stress in bacterial adaptation.

MATERIAL AND METHODS

Bacterial strains and media

Bacterial strains and media are described in additional materials.

Plasmids

Plasmids used in these studies are described in Table S1. Primers used for the plasmid constructions were obtained from Sigma-Aldrich (France) and are listed in Table S2.

***In vivo* recombination assays**

The suicide conjugation assay and recombination assay in replicative conditions are described in additional materials and in Bouvier et al, 2005.

Recombination assay with unidirectional replicative substrate

In this assay, the two natural *attC_{aadA7}* and *VCR_{2/1}* sites were used to analyze the effect of replication on integron recombination. To this end, we constructed two unidirectional replicating pTSC plasmids carrying the *attC* sites in either of the two orientations. A thermosensitive origin was chosen (oriPSC101ts). Each pTSC::*attC* plasmid was introduced in a UB5201 strain containing the pBAD::*IntI1* plasmid and the pSU38Δ::*attI1* plasmid. The transformed cells were grown for 6h at 30°C (to allow pTSC::*attC* replication) in the presence of the respective antibiotics: Cm (pTSC::*attC* marker), Ap (pBAD::*IntI1* marker) and Km (pSU38Δ::*attI1* marker). The integrase was expressed by addition of 0.2% arabinose. Then, cells were plated at 42°C on Cm so that only the cells containing recombined pTSC::*attC*

could grow. 1% glucose was added to the plates to repress the pBAD promoter and prevent residual recombination events. The integration activity was calculated as the ratio of cells expressing the Cm^R marker to the total number of Ap^R Km^R clones.

Recombination assay with a non replicative substrate

This assay supplies the *attC* site on a double-stranded plasmid that cannot replicate once introduced into the recipient cell by transformation. For these, we transformed a *pir*⁻ strain (UB5201) containing the pBAD::*IntI1* and the pSU38Δ::*attI1* plasmids with 200ng of the pSW::*attC* plasmids. Competent cells were prepared in the presence of 0.2% arabinose to allow integrase expression. Transformants were selected on Cm^R (the pSW::*attC* marker). As pSW::*attC* cannot replicate in the UB5201 strain, Cm^R clones correspond to *attC* x *attI* recombination events. To establish the recombination activity, we in parallel transformed a *pir*⁺ strain (UB5201-Pi), which allows the replication of the pSW::*attC* plasmids. Transformants were selected for Cm^R (the pSW::*attC* marker). The recombination activity corresponds to the ratio of Cm^R clones obtained in *pir*⁻ conditions to those obtained in *pir*⁺ conditions. Note that the efficiency of each *pir*⁺ and *pir*⁻ UB5201 strains was determined and the final ratio was adjusted. To study the effect of superhelicity, we performed this assay in JTT1 and SD7 strains. We also transformed these two strains by using substrates treated with the topoisomerase I. Note that the same quantity (200 ng) of treated and untreated plasmids were used to transform UB5201, UB5201-Pi , JTT1 and SD7 strains.

Topoisomers production

See the additional materials.

***In vitro* detection of cruciform**

Potential cruciform loops on the pSW::*attC_{aadA7}* and pSW::*VCR_{2/1}* plasmids were detected by S1 nuclease sensitivity and digested with NcoI or BglII for pSW::*attC_{aadA7}* and NcoI or ScaI for pSW::*VCR_{2/1}* (additional materials).

Analysis of recombination events and point localization

Note for all the recombination assays, recombination frequencies correspond to the average of at least three independent trials. Recombination events were checked by Polymerase chain reaction and the recombination point was precisely determined by sequencing (Bouvier et al, 2005 and additional materials).

Calculation of the probability to form active *attC* sites from single-stranded DNA

UNAFold software was used to compute the probability to form active *attC* sites from single-stranded DNA. We consider that to be folded properly, *attC* sites need to form the R'/R'' and L'/L'' boxes (Figure 1). A proper L'/L'' box is characterized by the presence of the extrahelical G16. We can observe that it is sufficient to constrain the pairing of A17 for the proper fold to be energetically the most favorable. We thus looked at the probability to pair the A17 properly without constraints using the hybrid-ss function of UNAFold. We consider this probability to be a reasonable estimate of the probability to form active *attC* sites from single-stranded DNA.

ACKNOWLEDGMENTS

The authors acknowledge Dean Rowe-Magnus and Priscilla des Gachons for critical reading of the manuscript. This study was carried out with financial assistance from the Institut Pasteur, the Centre National de la Recherche Scientifique (CNRS-URA 2171), the French National Research Agency (ANR-08-MIE-016), the EU (STREP CRAB, LSHM-CT-2005-019023, and NoE EuroPathoGenomics, LSHB-CT-2005-512061) and the Fondation pour la Recherche Médicale (programme “équipe FRM” 2007).

Conflict of interest

The authors declare that they have no conflict of interest.

SUPPLEMENTARY INFORMATION is available at The EMBO Journal Online.

REFERENCES

- Azaro, M.A. and Landy, A. (2002) Chapter 7 - λ integrase and the λ Int family. In Craig, N.L., Craigie, R., Gellert, M. and Lambowitz, A.M. (eds.), *mobile DNA II*. ASM Press, Washington, DC, pp. 118-148.
- Bacolla, A. and Wells, R.D. (2004) Non-B DNA conformations, genomic rearrangements, and human disease. *J Biol Chem*, **279**, 47411-47414.
- Balke, V.L. and Gralla, J.D. (1987) Changes in the linking number of supercoiled DNA accompany growth transitions in Escherichia coli. *J Bacteriol*, **169**, 4499-4506.
- Bierne, H., Ehrlich, S.D. and Michel, B. (1997) Deletions at stalled replication forks occur by two different pathways. *Embo J*, **16**, 3332-3340.
- Boucher, Y., Nesbo, C.L., Joss, M.J., Robinson, A., Mabbutt, B.C., Gillings, M.R., Doolittle, W.F. and Stokes, H.W. (2006) Recovery and evolutionary analysis of complete integron gene cassette arrays from Vibrio. *BMC Evol Biol*, **6**, 3.
- Bouvier, M., Demarre, G. and Mazel, D. (2005) Integron cassette insertion: a recombination process involving a folded single strand substrate. *Embo J*, **24**, 4356-4367.
- Bouvier, M., Ducos-Galand, M., Loot, C., Bikard, D. and Mazel, D. (2009) Structural features of single-stranded integron cassette attC sites and their role in strand selection. *PLoS Genet*, **5**, e1000632.
- Champion, K. and Higgins, N.P. (2007) Growth rate toxicity phenotypes and homeostatic supercoil control differentiate Escherichia coli from Salmonella enterica serovar Typhimurium. *J Bacteriol*, **189**, 5839-5849.

- Collis, C.M., Recchia, G.D., Kim, M.J., Stokes, H.W. and Hall, R.M. (2001) Efficiency of recombination reactions catalyzed by class 1 integron integrase IntI1. *J Bacteriol*, **183**, 2535-2542.
- d'Alencon, E., Petranovic, M., Michel, B., Noiro, P., Aucouturier, A., Uzest, M. and Ehrlich, S.D. (1994) Copy-choice illegitimate DNA recombination revisited. *Embo J*, **13**, 2725-2734.
- Dai, X. and Rothman-Denes, L.B. (1999) DNA structure and transcription. *Curr Opin Microbiol*, **2**, 126-130.
- Francia, M.V., Zabala, J.C., de la Cruz, F. and Garcia-Lobo, J.M. (1999) The IntI1 integron integrase preferentially binds single-stranded DNA of the *attC* site. *Journal of Bacteriology*, **181**, 6844-6849.
- Frumerie, C., Ducos-Galand, M., Gopaul, D.N. and Mazel, D. (2009) The relaxed requirements of the integron cleavage site allow predictable changes in integron target specificity. *Nucleic Acids Res.*
- Gamper, H.B. and Hearst, J.E. (1982) A topological model for transcription based on unwinding angle analysis of E. coli RNA polymerase binary, initiation and ternary complexes. *Cell*, **29**, 81-90.
- Guasch, A., Lucas, M., Moncalian, G., Cabezas, M., Perez-Luque, R., Gomis-Ruth, F.X., de la Cruz, F. and Coll, M. (2003) Recognition and processing of the origin of transfer DNA by conjugative relaxase TrwC. *Nat Struct Biol*, **10**, 1002-1010.
- Guerin, E., Cambay, G., Sanchez-Alberola, N., Campoy, S., Erill, I., Da Re, S., Gonzalez-Zorn, B., Barbe, J., Ploy, M.C. and Mazel, D. (2009) The SOS response controls integron recombination. *Science*, **324**, 1034.

- Guynet, C., Hickman, A.B., Barabas, O., Dyda, F., Chandler, M. and Ton-Hoang, B. (2008) In vitro reconstitution of a single-stranded transposition mechanism of IS608. *Mol Cell*, **29**, 302-312.
- Hall, R.M., Brookes, D.E. and Stokes, H.W. (1991) Site-specific insertion of genes into integrons: role of the 59-base element and determination of the recombination cross-over point. *Mol Microbiol*, **5**, 1941-1959.
- Hall, R.M. and Collis, C.M. (1995) Mobile gene cassettes and integrons: capture and spread of genes by site-specific recombination. *Molecular Microbiology*, **15**, 593-600.
- Hartvig, L. and Christiansen, J. (1996) Intrinsic termination of T7 RNA polymerase mediated by either RNA or DNA. *Embo J*, **15**, 4767-4774.
- Jaworski, A., Higgins, N.P., Wells, R.D. and Zacharias, W. (1991) Topoisomerase mutants and physiological conditions control supercoiling and Z-DNA formation in vivo. *J Biol Chem*, **266**, 2576-2581.
- Khan, S.A. (2005) Plasmid rolling-circle replication: highlights of two decades of research. *Plasmid*, **53**, 126-136.
- Leach, D.R. (1994) Long DNA palindromes, cruciform structures, genetic instability and secondary structure repair. *Bioessays*, **16**, 893-900.
- Lilley, D.M. (1980) The inverted repeat as a recognizable structural feature in supercoiled DNA molecules. *Proc Natl Acad Sci U S A*, **77**, 6468-6472.
- Lilley, D.M., Gough, G.W., Hallam, L.R. and Sullivan, K.M. (1985) The physical chemistry of cruciform structures in supercoiled DNA molecules. *Biochimie*, **67**, 697-706.
- Lodge, J.K., Kazic, T. and Berg, D.E. (1989) Formation of supercoiling domains in plasmid pBR322. *J Bacteriol*, **171**, 2181-2187.
- MacDonald, D., Demarre, G., Bouvier, M., Mazel, D. and Gopaul, D.N. (2006) Structural basis for broad DNA specificity in integron recombination. *Nature*, **440**, 1157-1162.

- Mazel, D. (2006) Integrons: agents of bacterial evolution. *Nat Rev Microbiol*, **4**, 608-620.
- Napierala, M., Bacolla, A. and Wells, R.D. (2005) Increased negative superhelical density in vivo enhances the genetic instability of triplet repeat sequences. *J Biol Chem*, **280**, 37366-37376.
- Noirot, P., Bargonetti, J. and Novick, R.P. (1990) Initiation of rolling-circle replication in pT181 plasmid: initiator protein enhances cruciform extrusion at the origin. *Proc Natl Acad Sci U S A*, **87**, 8560-8564.
- Pages, V. and Fuchs, R.P. (2003) Uncoupling of leading- and lagging-strand DNA replication during lesion bypass in vivo. *Science*, **300**, 1300-1303.
- Panayotatos, N. and Wells, R.D. (1981) Cruciform structures in supercoiled DNA. *Nature*, **289**, 466-470.
- Prudhomme, M., Attaiech, L., Sanchez, G., Martin, B. and Claverys, J.P. (2006) Antibiotic stress induces genetic transformability in the human pathogen *Streptococcus pneumoniae*. *Science*, **313**, 89-92.
- Pruss, G.J. and Drlica, K. (1986) Topoisomerase I mutants: the gene on pBR322 that encodes resistance to tetracycline affects plasmid DNA supercoiling. *Proc Natl Acad Sci U S A*, **83**, 8952-8956.
- Robleto, E.A., Yasbin, R., Ross, C. and Pedraza-Reyes, M. (2007) Stationary phase mutagenesis in *B. subtilis*: a paradigm to study genetic diversity programs in cells under stress. *Crit Rev Biochem Mol Biol*, **42**, 327-339.
- Rowe-Magnus, D.A., Guerout, A.M., Biskri, L., Bouige, P. and Mazel, D. (2003) Comparative analysis of superintegrons: engineering extensive genetic diversity in the vibrionaceae. *Genome Res*, **13**, 428-442.

- Stokes, H.W., O'Gorman, D.B., Recchia, G.D., Parsekhian, M. and Hall, R.M. (1997) Structure and function of 59-base element recombination sites associated with mobile gene cassettes. *Molecular Microbiology*, **26**, 731-745.
- Ton-Hoang, B., Guynet, C., Ronning, D.R., Cointin-Marty, B., Dyda, F. and Chandler, M. (2005) Transposition of ISHp608, member of an unusual family of bacterial insertion sequences. *Embo J*, **24**, 3325-3338.
- Trinh, T.Q. and Sinden, R.R. (1991) Preferential DNA secondary structure mutagenesis in the lagging strand of replication in *E. coli*. *Nature*, **352**, 544-547.
- Val, M.E., Bouvier, M., Campos, J., Sherratt, D., Cornet, F., Mazel, D. and Barre, F.X. (2005) The single-stranded genome of phage CTX is the form used for integration into the genome of *Vibrio cholerae*. *Mol Cell*, **19**, 559-566.

FIGURE LEGENDS

Figure 1: *attC* recombination sites.

A) Schematic representation of a double-stranded (ds) *attC* site. Inverted repeats R'', L'', L' and R' are indicated by grey boxes. The dotted line represents the variable central part. The conserved nucleotides are indicated. The asterisk (*) shows the conserved G nucleotide which generate an extrahelical base in the folded *attC* site bottom strand. The black arrow shows the cleavage point. B) Secondary structures of the VCR_{2/1} and *attC*_{aadA7} sites bottom strands (bs). Structures were determined by the MFOLD online interface at the Pasteur Institute. The sequences of the *attC* sites are indicated except for the VTS of the VCR_{2/1} site.

Figure 2: Cellular processes possibly allowing the *attC* site folding.

The different possible cellular pathways allowing proper folding of the *attC* site bottom strand: from single-stranded DNA during replication and conjugation, and cruciform

extrusion from supercoiled double-stranded DNA. IntI monomers are represented as grey ovals.

Figure 3: Influence of processes delivering single-stranded DNA on *attC* recombination.

A) Recombination frequencies of the different *attC* sites in the “suicide-conjugation” assay as a function of their probability to fold a recombinogenic *attC* site. The UNAFold software was used (see Experimental procedures). B) Recombination frequencies of four natural *attC* sites after conjugation in either a replication permissive [pir+] or non-permissive [pir-] recipient (see Experimental procedures). Black and white columns correspond respectively to the recombination frequencies established when the bottom strand (bs) or the top strand (ts) is injected by conjugation. C) Recombination frequencies of the VCR_{2/1} and *attC*_{aadA7} when the recombinogenic bs is carried on the lagging (lag) or leading (lead) strand of the replicating molecule. Error bars show standard deviations.

Figure 4: *attC* recombination, in “replicative” recombination conditions.

A) Recombination frequencies of the different *attC* sites in the “replicative” assay as a function of their VTS size. Error bars show standard deviations. B) Secondary structures of *attC*_{97a} and *attC*_{97b} as predicted by MFOLD. G:C and A:T base pairs are marked respectively by red and blue dashes. The 5' and 3' ends are indicated and bases are numbered. The free energy of cruciform formation (ΔG), the probability to fold a recombinogenic *attC* site and its measured recombination frequencies are indicated for each site.

Figure 5: Extrusion of the *attC* sites secondary structures from double-stranded DNA.

A) Schemes of the plasmids with extruded *attC* sites and the expected S1 fragments sizes (in bp) after cleavage by the different restriction enzymes. B) *In vitro* mapping of S1 nuclease-

sensitive sites. S1 treated (+) or untreated (-) plasmids, were subjected to restriction digest (enzymes are indicated above each lane) and submitted to electrophoresis. The bands (white asterisks) smaller than the linear monomer (lin) result from S1 nuclease action and thus of cruciform extrusion. Kb: marker DNA. C) Recombination frequencies of different *attC* sites in the “non replicative” recombination assay. Error bars show standard deviations. D) Energy landscape of cruciform formation. Each color dot represents the free energy of cruciform formation (ΔG_c in Kcal.mol⁻¹) for a portion of the *attC* site of length *w* (bp) at the position *p* (from favorable in blue to unfavorable in red). The tip of the triangle is the free energy of the whole *attC* site. Since *attC* sites are symmetrical, favorable energies that are not along the center of the triangle represent favorable non-recombinogenic structures. *attC_{aadA7}* folds in a favorable recombinogenic site (blue color from the middle of the base of the triangle). VCR_{2/1} folds in a favorable non-recombinogenic structure (blue color shifted from the middle).

Figure 6: Influence of superhelicity on *attC* folding.

A) Mapping of S1 nuclease-sensitive sites of topoisomers products. Topoisomerase I treatment (+) of the plasmids, or not (-), and restriction enzymes used are mentioned above the lanes. The estimated band sizes for the extrusion of *attC_{aadA7}* and VCR_{2/1} in the pSW plasmid are given in figure 5A. Kb: marker DNA B). Effect of topoisomerase I activity on the recombination propensity of the *attC_{aadA7}* site. “non replicative” recombination assay were performed in two genetic backgrounds, wild type (WT) and *topA10gyrB266* (topgyr, topoisomerase I and DNA gyrase deficient strain). Error bars show standard deviations.

Figure 7: Model for the *attC* site folding pathways.

The single-stranded and double-stranded pathways involving respectively replication and conjugation processes, and cruciform extrusion are represented. The double-stranded

pathway is composed of the C and S-type cruciform pathways (Lilley et al., 1985). The C-type implicates a single step process requiring the denaturation of the entire inverted repeat and snap-back to form the intra-strand-bonded cruciform structure. The S-type implicates a multi-step process in which the initial melted “bubble” is extended by branch migration.

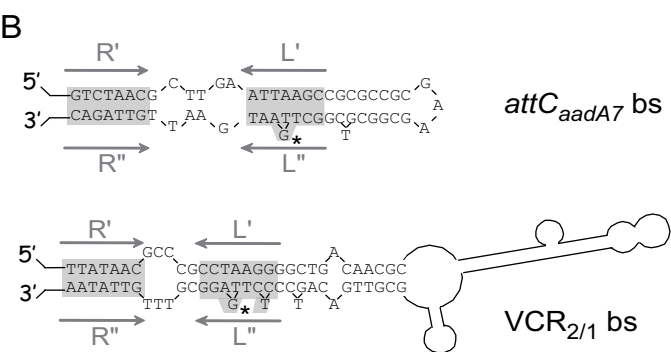
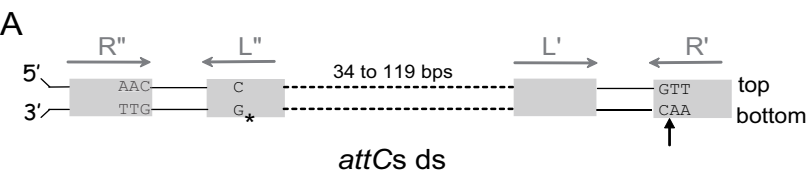


Figure 1

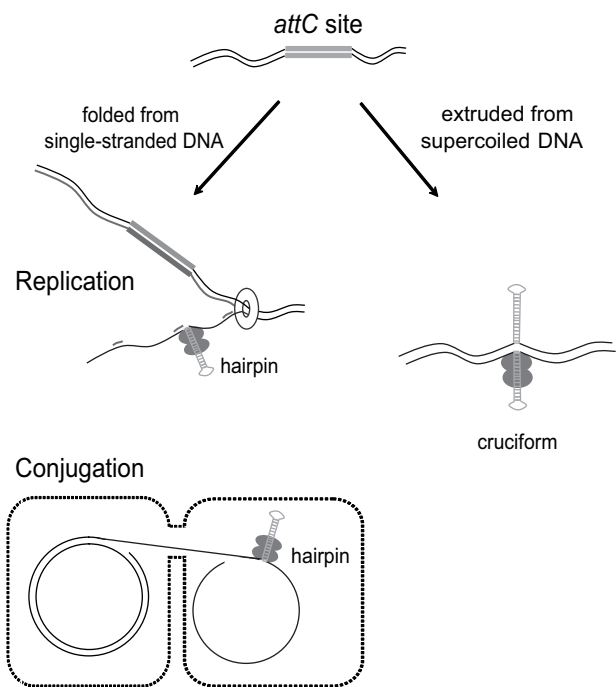


Figure 2

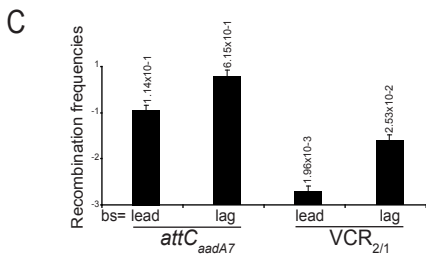
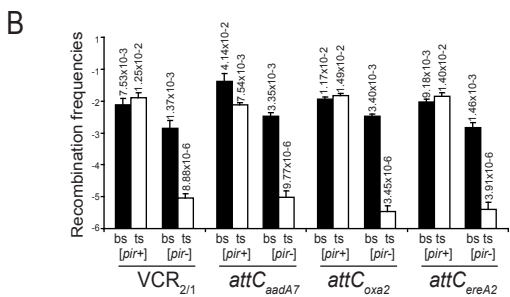
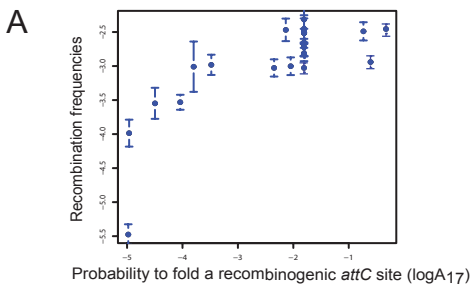


Figure 3

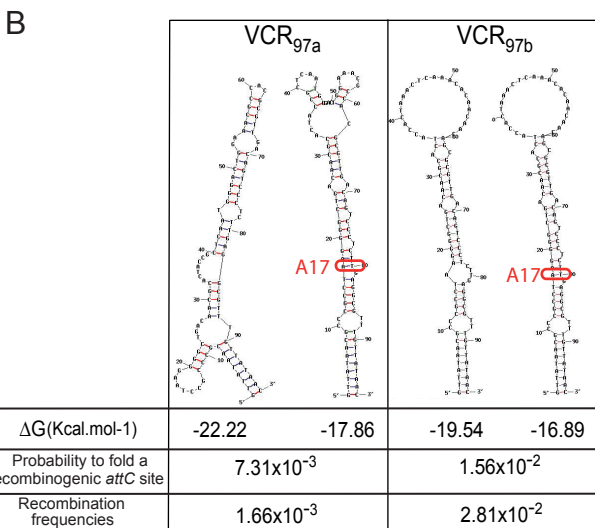
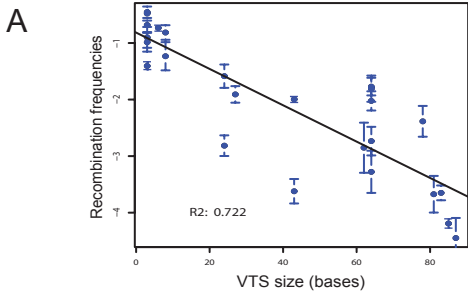


Figure 4

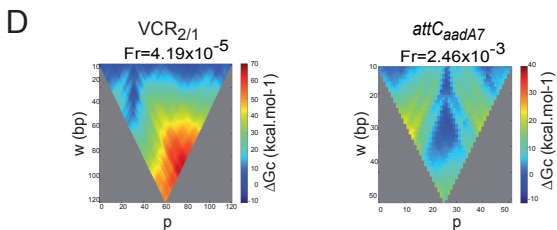
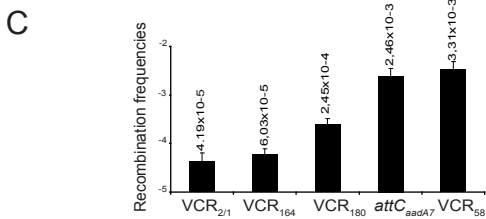
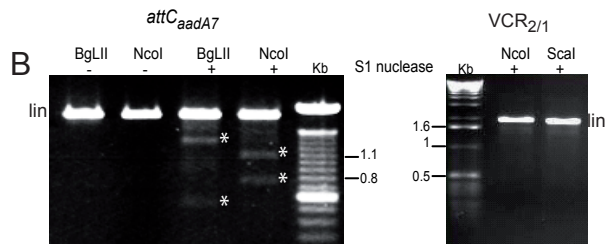
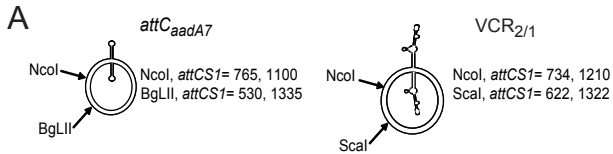


Figure 5

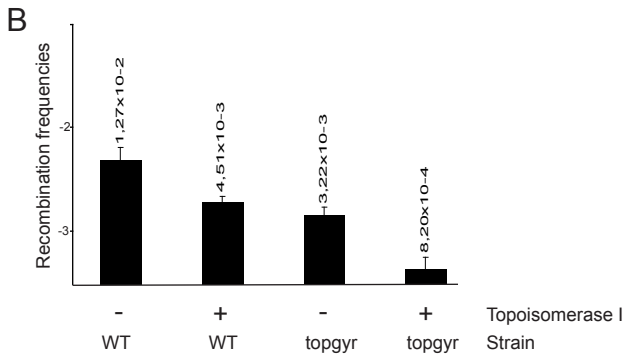
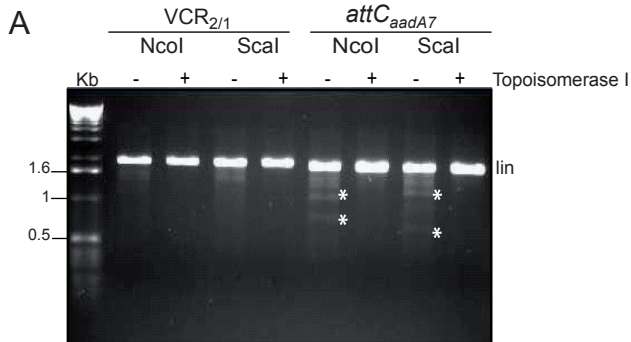


Figure 6

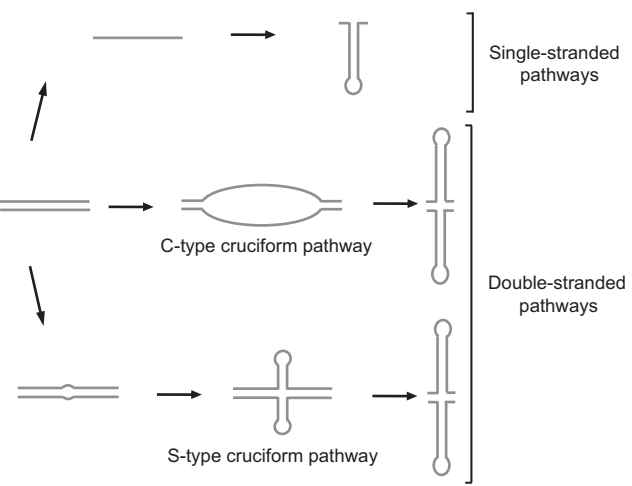


Figure 7